Identification of the Root Canal from Dental Micro-CT Records*

László Szilágyi[1,2], Csaba Dobó-Nagy[3], and Balázs Benyó[1]

[1] Budapest University of Technology and Economics, Department of Control Engineering and Information Technology, Budapest, Hungary
[2] Sapientia - Hungarian Science University of Transylvania, Faculty of Technical and Human Science, Tîrgu-Mureş, Romania
lalo@ms.sapientia.ro
[3] Semmelweis University, Independent Section of Radiology, Budapest, Hungary

Abstract. This paper presents a novel semi-automated image processing procedure dedicated to the identification and characterization of the dental root canal, based on high-resolution micro-CT records. After the necessary image enhancement, parallel slices are individually segmented via histogram based quick fuzzy c-means clustering. The 3D model of root canal is built up from the segmented cross sections using the reconstruction of the inner surface, and the medial line is extracted by a 3D curve skeletonization algorithm. The central line of the root canal can finally be approximated as a 3D spline curve. The proposed procedure may support the planning of several kinds of endodontic interventions.

Keywords: image processing, skeleton extraction, micro computed tomography, fuzzy c-means algorithm.

1 Introduction

The ability to localize all canals within a tooth is essential for rendering successful endodontic treatment and for ensuring long term successful outcome. In the process, it is necessary to minimize risks and untoward sequelae associated with treatment of challenging teeth. For example, severely curved or multiple curved canals may pose diagnostic and treatment challenge. The new imaging technologies such as CBCT show great promise to ascertain, before endodontic treatment is commenced. Since this novel modality provides digitized images in 3D, this raw data of the set of voxels serves as a basis of further analysis. In order to make the system more efficient and effective, the work of our interdisciplinary research group focuses on the automatic recognition of the root and root canals and mathematical description of root canal curvatures, as well. The integration of these steps of image processing in novel systems may significantly improve the

* This project is supported in part by the New Széchenyi Plan (Project ID: TÁMOP-4.2.1/B-09/1/KMR-2010-0002), and the Hungarian National Scientific Research Foundation, Grants No. T80316 and T82066. The work of L. Szilágyi was supported by János Bolyai Fellowship Program of the Hungarian Academy of Sciences.

C. San Martin and S.-W. Kim (Eds.): CIARP 2011, LNCS 7042, pp. 339–346, 2011.
© Springer-Verlag Berlin Heidelberg 2011

endodontic practice in the near future. Also, the attempt to automatically locate and classify the root canals may result in significantly decreased chair time for both the patient and the practitioner.

Root canals differ from individual to individual and from tooth to tooth. That is why whenever an endodontic intervention is planned, the shape of that given root canal needs to be accurately detected. Modern medical imaging devices make it possible to record high resolution cross sections of the teeth, which can be fed to image processing techniques to extract the shape of the root canal. This problem has been solved several different ways, based on recorded data originating from various imaging tools.

Analui et al [1] elaborated a geometric approach for modeling and measurement of root canal of human dentition based on stereo digital radiography. Hong et al [6] used both 2D radiographic and endoscopic images to build up a 3D tooth model, while Endo et al [4] turned to ultrasonic imaging and implemented a fuzzy logic based root canal detection. Lee et al [7] used micro CT images and a 3D reconstruction software to measure the three-dimensional canal curvature in maxillary first molars via mathematical modeling.

Recently, several other 3D dental structure reconstruction systems were elaborated, including Willerhausen et al [11] who used X-ray images, and Van Soest et al [8], who applied optical coherence tomography records for 3D structure reconstruction. Germans et al [5] presented an imaging system based on virtual reality that can navigate through the reconstructed 3D structure and make measurements concerning the curvature of the root canal. An excellent review of current researches based on micro-CT data can be found in [9].

In this paper we introduce a complete image processing procedure, which starts with the enhancement of input micro CT slices, continues with 2D image segmentation based on an enhanced fuzzy c-means clustering [10], identification of the root center in 2D slices via a region growing method. At this point the algorithm can bifurcate: we can interpolate the 3D shape of the root canal's medial axis from the centers detected in 2D, or we can build a 3D tubular shape model and extract the medial axis using 3D morphological operations.

2 Background Works: 3D Curve Skeleton Extraction

In two dimensions, the skeleton of an object is defined as the union of locations that possess at least two closest points on the boundary of the object. These places are usually localized using the grass-fire algorithm or the method of largest circles. The straightforward extension of these algorithms to 3D objects produces skeletons consisting of medially placed curves and surfaces. As several computer graphics applications demanded the concise representation of 3D objects with curve arcs, the notion of 3D curve skeleton was introduced, having no mathematical definition, but sharing a series of specific properties [3].

In the followings, we will shortly introduce the 3D curve skeleton extraction methods and discuss only those specific properties, which are relevant in our application. Methods based on thinning or boundary propagation iteratively

remove so-called simple points (whose presence does not affect the topology), from the surface of the object. This is generally achieved using a hit-or-miss transform extended to three dimensions. Approaches based on distance fields define and compute the minimum distance of each discrete interior point to the surface of the object, an approximate the curve skeleton with the ridges of this distance field. Geometric models generally use a graph-based representation the approximation of the medial surface or curve of the object. Generalized potential field methods define an internal potential field that differs from the distance field (e.g. electrostatic field generated by placing point charges to all discrete boundary locations [2]), and extract a hierarchical structure composed of critical and saddle points of the field.

Being a straightforward extension of 2D skeletons, 3D curve skeletons are also composed of loci having at least two closest points on the boundary of the object. This property makes curve skeletons suitable to approximate the center line of the root canal. Curve skeletons preserve the topology of the object, and embody the hierarchy of its components, which is relevant at the detection of bifurcations. In order to suit the needs of our application, we have to choose the approach that yields the smoothest curve and performs the least sensitive to slight changes of the object boundary. As we will see later, these latter conditions are most suited by the potential field approach.

For further details on the topic of 3D curve skeletons, the reader is referred to [3], which is an excellent repository of such methods and their properties.

3 Methods

Dental micro CT records consist of single channel intensity images, representing high-resolution (1500-3000dpi) scans of parallel cross sections of a certain tooth. A set of images may contain several hundreds of scanned horizontal planes, which usually are linearly distributed along an axis that is orthogonal to the scanned planes. The distribution of pixel intensity levels varies from slice to slice, but there are a few rules which most slices obey. In this order, the anatomical structure is reflected by pixel intensities. In normal cases, cross sections contain a light gray spot corresponding to the dentin, usually lighter at its edges (that is because the enamel) with circularly distributed texture due to imaging artifacts, possibly surrounding one or more darker regions, which represent the root canal containing soft tissues. The cementum, when visible, is usually somewhat lighter than the dentin.

The main goal of our image processing procedure is to identify the 3D structure of the root canal that we can build up from the inner darker regions identified from all cross sections. Afterwards, we need to track the spatial curve that corresponds to the central line. The detected central line must follow the topology of the root canal, by reflecting its curves and bifurcations.

Figure 1(left) exhibits the diagram of the image processing procedure. The following paragraphs discuss the functionality of each box of the diagram.

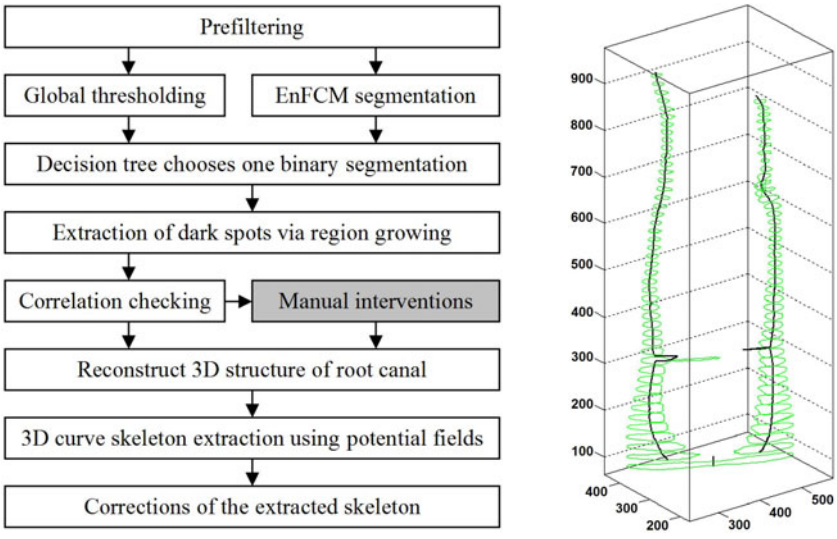

Fig. 1. (left) The steps of the proposed algorithm; (right) Checking the correlation of dark spot centers in neighbor slices reveal the presence of bifurcations (around slice 70) and the need for manual interaction (around slice 310). Both events can be localized and identified automatically.

Preprocessing. The automatic image segmentation must be preceded by some image enhancement steps. In our application, the following preprocessing steps are employed: (1) A simple median filter, which reduces the high frequency noise that is most visible in the dentin's texture; (2) Establishing the region of interest (ROI) by trimming the image: this way we get rid of the dark areas that represent outer space. It is necessary to store the exact coordinates of the ROI; (3) Some basic morphological operators are used to remove texts from the original image and regularize the boundary of the root canal.

Segmentation in 2D. The final result of the planar segmentation should be a binary image. Even if the image enhancement techniques have already suppressed the disturbing textures, in order to assure high quality segmentation, we need to apply a double partitioning and combine their outcome.

In this order, this phase produces two different partitions that are both obtained using the enhanced FCM (EnFCM) clustering algorithm [10]. The first partition is achieved by performing EnFCM on the ROI of the slice, setting the number of clusters to $c = 4$. In the followings, this partition will be referred to as local partition, as it is computed from the local data of the slice. The second partition is produced by a simple thresholding operation, using a previously computed threshold τ_{global} that was obtained by EnFCM from the whole dataset, using $c = 2$ clusters. This latter partition is called global partition of the slice, because it uses the global threshold extracted from the data of all slices. As the matter of fact, not all slices contribute to the global threshold: only a representative selection of slices is taken

into consideration, in order to reduce computation time. The global threshold produces a binary image at once. The local partition contains 4 different colors, corresponding to the prototypes of the 4 clusters, v_1 to v_4. Let us suppose the intensity values are ordered increasingly, that is, $v_{i+1} > v_i$, $\forall i = 1 \dots c-1$. The 4 clusters are then separated in two classes, using the threshold $\tau_{\text{local}} = (v_{i+1} - v_i)/2$, where $i = \arg\max_j \{v_{j+1} - v_j, j = 1 \dots c-1\}$. In most cases, both binary images are good quality partitions, but there are exceptions, when one of these algorithms fails. In these cases we need to select the correct partition.

Decision making. In order to provide an intelligent selection of the correct binary partition, we have built up a decision tree, based on 250 slices representing above mentioned exceptions. The decision is made in a four dimensional search space, corresponding to parameters: τ_{global}, and $\tau_i = (v_{i+1} - v_i)/2$, where $i = 1 \dots 3$. The output of the tree is the decision whether the local or the global binary partition is the correct one. During the training process, we employed the entropy minimization technique until all leaves of the tree became homogeneous. After having the decision tree trained, the decision can be made quickly. Finally we obtain a binary image, where the inner dark regions have to be localized.

Region growing and selection. The identification of dark spots situated within the light area of the binary image, is performed by an iterative region growing method. As long as there are dark pixels in the segmented image, a dark pixel is arbitrarily chosen and a region is grown around it. Outer space (which is also dark) is obviously discarded, and the detected dark spots are separately stored. Each branch of the root canal, which is present in the cross section, should normally be represented by a single dark region within the slice. Unfortunately, mostly because of imaging artifacts or complex shaped canals, there are some cases, when a single canal branch is manifested by more than one dark region. These cases can be detected automatically, but their treatment sometimes requires manual interventions.

Each dark spot has its center point, which we can compute two different ways: as the center of gravity of the spot, or by the means of morphological thinning. The center of gravity is easier to compute, but sometimes it falls outside the spot. Morphological thinning always gives a quasi centrally located center point, but it brings more computational load.

The automatic selection of detected spots can be performed by several different protocols, which are: P1 – always extracts the largest dark spot from the slice; P2 – also extracts the second/third/fourth largest spot if it is present and is larger than a small threshold size; P3 – adaptive, which may extract any number of spots, according to some predefined rules that concern the size of different spots. Protocol P1 can be used in cases of incisor teeth only, when a priori anatomical information makes the presence of a single spot highly probable.

Automatic shape regularization. Due to the artifacts present in the original microCT records, the dark spot detected in certain slices may contain irregularities. There are several kinds of such cases: some can be treated by automatic regularization techniques, while there are also cases that require manual

interaction. For example, a light "island" within the dark spot is easily removable. Strange shaped "peninsulas" can be treated by large masked median filter or morphological opening/closing. There are also cases where the real root canal is detected as several separate dark spots situated very close from each other, which need to be unified. Automatic unification is possible using morphological operations or distance transform.

Correlation checking. The accurate segmentation of the microCT images may demand manual intervention. Luckily, the necessity of such steps is visible from the correlation of detected dark spots within adjacent cross sections, or in other words, there cannot be a relevant change in the structure found within neighbor slices. Wherever there is a large distance between the center points detected in neighbor slices, either we have a bifurcation, or some intervention is likely to be beneficial. In case of bifurcation, the number of dark spots in the neighbor slices should differ, but correlate with the other neighbors of each.

Manual interactions to improve accuracy. The user has the opportunity to change the result of the automatic segmentation within any of the slices. As it was justified in the previous section, the user is advised where the interaction is required. The implemented manual interventions are: M1 – overrule the decision dictated by the decision tree; M2 – Change the local threshold to any desired value; M3 – discard some of the automatically detected dark spots; M4 – unify several dark spots using a parametric active contour model (snake).

Reconstruct the spatial shape of the root canal. The inner dark spots localized within each slice are put together in space to form a three dimensional object that describes the shape of the root canal. The center line of this object will be searched for using a procedure based on 3D curve skeleton extraction.

3D curve skeleton extraction. As mentioned in [3], there are various approximation algorithms for the 3D curve skeleton of voxelized objects. We need to employ such an approach which provides a smooth curve with low amount of branches, and extremely insensitive to zigzagged surfaces. This sort of curve skeleton is reportedly produced by potential field methods. We have successfully implemented the method proposed in [2], and applied it to extract the skeletons of the root canal object.

Corrections of the extracted skeleton. The 3D curve skeleton accurately handles critical cases like root canal bifurcations, or slices that are far from being orthogonal to the root canal's direction. Under such circumstances, the curve skeleton is an excellent approximation of the center line. However, at all endings of the root canal, the curve skeleton is either shorter than it should be as the iterative thinning has its effect from every direction, or it has several short branches connected to high curvature points of the surface of the reconstructed 3D object. In order to produce an accurate center line with the skeleton extraction algorithm, we need to choose the divergence parameter of Cornea's potential field approach low enough, so that the endings of the skeleton towards superficial high curvature points are not present. Further on, in order to avoid

the shortened endings of the skeleton, we need to virtually lengthen all endings of the reconstructed tubular 3D object with as many slices (identical to the peripheral one) as necessary. The number of such virtually added slices is well approximated as the shortest radius of the dark spot in the peripheral slice.

Most steps of the algorithm summarized in Fig. 1(left) are performed automatically. The only box having gray background represents a step that requires manual interaction. This step is not mandatory in simple cases, e.g. incisor teeth on images with low amount of artifacts.

4 Results and Discussion

The proposed algorithm can automatically process more than 95% of the recorded image sets, while the rest of the cases need manual interaction. Using a Pentium4 PC, the processing of a slice in 2D lasts 0.3-0.5 seconds, while a central canal reconstruction is interpolated in less than a second. The accuracy of the detected medial axis also depends on the number of slices involved. An accuracy that is suitable to guide medical intervention can be obtained from carefully selected subsets of at least 50 slices.

Figure 2(left) exhibits the intermediary results provided by the 2D segmentation. Three cases of various difficulties are presented in the three rows of the image. The first row presents a simple case involving a slice with two dark spots representing two different, easily detectable root canals (there was a bifurcation several slices away from this one). The slice in the middle row manifests an odd shaped dark region, which was successfully detected. The slice presented in the

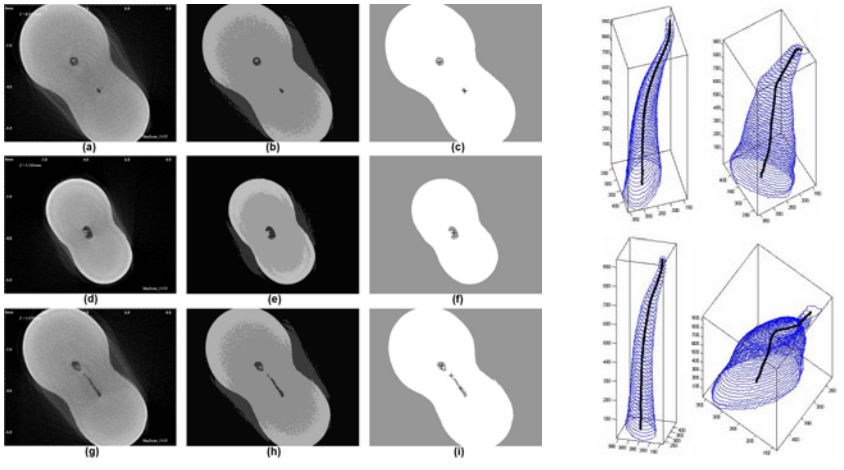

Fig. 2. (left) Detailed view of image segmentation in 2D: each row represents a different slice. First column shows the original recorded images; second column presents the clustered images (4 clusters); last column indicates the segmented binary images with detected center points; (right) 3D views of a root canal, with the extracted medial line. Numbers indicate pixels, which are easily convertible to millimeters.

third row shows a difficult case: three different dark spots are present in the segmented images, but they belong to only two different canal branches. This is the case which requires correlation test with neighbors or decision overruling performed by the ANN.

Figure 2(right) shows four different 3D views of a root canal, together with its detected medial axis. The central line was produced from 944 equidistant slices, segmented in 2D with binary separation using the global optimal threshold.

5 Conclusions

We have proposed and implemented a complex image processing procedure for the detection of the center line from dental micro CT records. In most cases the algorithm performs automatically, but there are still a few nodes in the decision tree where the decision has to be made interactively. Thus we have created an imaging system that can efficiently assist certain medical interventions.

References

1. Analoui, M., Krisnamurthy, S., Brown, C.: Modeling and measurement of root canal using stereo digital radiography. In: Proceedings of SPIE - The International Society for Optical Engineering, vol. 3976, pp. 306–314 (2000)
2. Cornea, N.D., Silver, D., Yuan, X., Balasubramanian, R.: Computing hierarchical curve-skeletons of 3D objects. The Visual Computer 21, 945–955 (2005)
3. Cornea, N.D., Silver, D., Min, P.: Curve-skeleton properties, applications, and algorithms. IEEE Trans. Vis. Comp. Graph. 13, 530–548 (2007)
4. Endo, M., Kobashi, S., Kondo, K., Hata, Y.: Dentistry support ultrasonic system for root canal treatment aided by fuzzy logic. In: Proceedings of IEEE International Conference on Systems, Man and Cybernetics, vol. 2, pp. 1494–1499 (2005)
5. Germans, D.M., Spoelder, H.J.W., Renambot, L., Bal, H.E., van Daatselaar, S., van der Stelt, P.: Measuring in virtual reality: a case study in dentistry. IEEE Trans. Instrum. Meas. 57, 1177–1184 (2008)
6. Hong, S.Y., Dong, J.: 3-D root canal modeling for advanced endodontic treatment. In: Progress in Biomedical Optics and Imaging - Proceedings of SPIE - The International Society for Optical Engineering, vol. 4702, pp. 321–330 (2002)
7. Lee, J.K., Ha, B.H., Choi, J.H., Perinpanayagam, H.: Quantitative three-dimensional analysis of root canal curvature in maxillary first molars using micro-computed tomography. J. Endodontics 32, 941–945 (2006)
8. van Soest, G., Shemesh, H., Wu, M.K., van der Sluis, L.W.M., Wesselink, P.R.: Optical coherence tomography for endodontic imaging. In: Progress in Biomedical Optics and Imaging - Proceedings of SPIE 6843, vol. 6843, art. no. 68430F, pp. 1–8 (2008)
9. Swain, M.V., Xue, J.: State of the art of micro-CT applications in dental research. Int. J. Oral. Sci. 1, 177–188 (2009)
10. Szilágyi, L., Benyó, Z., Szilágyi, S.M., Adam, H.S.: MR brain image segmentation using an enhanced fuzzy c-means algorithm. In: 25th Annual Int'l. Conference of IEEE Engineering in Medicine and Biology Society, pp. 724–726 (2003)
11. Willershausen, B., Kasaj, A., Röhrig, B., Marroquin, B.B.: Radiographic investigation of frequency and location of root canal curvatures in human mandibular anterior incisors in vitro. J. Endodontics 34, 152–156 (2008)